

Search for Magnetic Ordering in hcp Iron*

D. L. Williamson,† S. Bukshpan,‡ and R. Ingalls§

Department of Physics, University of Washington, Seattle, Washington 98105

(Received 18 April 1972)

Mössbauer spectroscopy has been used to study the effects of high pressure and low temperature on the properties of bcc and hcp metallic iron. There is considerable evidence which indicates hcp iron should order antiferromagnetically at low temperatures. A search was made to 20 °K at 148 kbar and 48 °K at 176 kbar. No evidence was found for magnetic ordering. However, the hcp-iron resonance line was definitely broader than the inner two bcc resonance lines at all temperatures. The latter can be accounted for by self-absorption broadening and a quadrupole splitting of 0.17 ± 0.03 mm/sec which is attributed to small quadrupole interactions in hcp iron. Results are presented on the pressure and temperature dependence of the isomer shift and second-order Doppler shift of bcc and hcp iron as well as on the hyperfine field of bcc iron. The effect of pressure on the second-order Doppler shift has been clearly observed and a characteristic Debye temperature of (545 ± 25) °K is found for hcp iron at 145 kbar. In addition, evidence is presented for a hysteresis associated with the bcc \rightarrow hcp transformation.

I. INTRODUCTION

Few materials have received as much theoretical, experimental, and practical interest as metallic iron. Despite the vast number of studies done, its microscopic properties are still not completely understood. Being a transition element, its magnetic properties are of primary interest.

Consider the pressure-temperature phase diagram¹⁻⁷ shown in Fig. 1. In the α (bcc) phase Fe is ferromagnetic except for the small region where, upon heating, the Curie transformation occurs before the α - γ (fcc) phase change. Understandably, α -Fe has received most of the attention. Recent band theories of α -Fe have reached the stage where many of the microscopic properties are qualitatively understood and quantitative agreement with experiment is achieved in some instances.⁸⁻¹⁰ One of the most important agreements is concerning the magnetic moment associated with each Fe atom ($2.2 \mu_B$) which was calculated with particularly careful treatment being given to the exchange interaction.⁹

The γ phase of Fe is paramagnetic in the pressure-temperature region depicted in Fig. 1. It should be noted, however, that precipitates of γ -Fe can be produced in Cu which are stable at low temperature. The latter are found to order antiferromagnetically below 70 °K with a hyperfine field of 24 kOe.^{11,12} Some information about the magnetic properties of γ -Fe has also been inferred from studies of Fe in fcc alloys.¹³⁻¹⁶ Only recently have detailed theories of fcc 3d transition metals appeared.^{17,18}

The high-pressure ϵ (hcp) phase of Fe was originally shown to be paramagnetic at room tem-

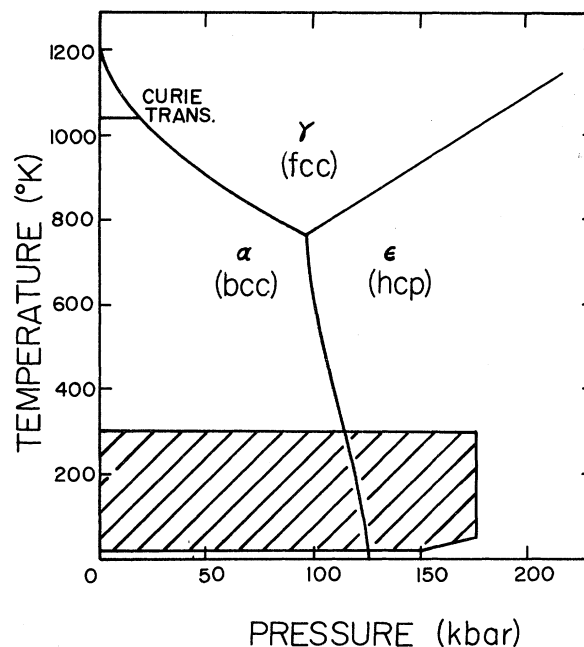


FIG. 1. Pressure-temperature phase diagram of metallic iron. Most of the diagram was determined by electrical resistance measurements using static pressure (Ref. 1) but the shape of the α - ϵ phase boundary below 300 °K was taken from shock wave measurements (Ref. 2). No data are available below 78 °K, and the curve is simply extrapolated to 0 °K. The Curie transformation data came from magnetic susceptibility studies (Ref. 3). The position of the α - ϵ phase boundary is at present still unsettled (Refs. 4-7). The latter stems partly from the apparent large hysteresis associated with the $\alpha \rightarrow \epsilon$ transitions (Ref. 7). In the above diagram the boundary has been adjusted to pass through 115 kbar at room temperature. The shaded area covers the present experiment.

perature using Mössbauer spectroscopy.^{19,20} One temperature study of ϵ -Fe has been done from room temperature to just above the triple point.²¹ This study using the Mössbauer effect also found no evidence of a magnetic phase.

Because of its inaccessibility, relatively little is known about ϵ -Fe in general.

The main impetus for the present experiment came from a suggestion that ϵ -Fe may have an antiferromagnetic phase at lower temperatures.²⁰ The suggestion is based upon the assumption that ϵ -Fe will behave similarly to γ -Fe. Recent studies²²⁻²⁴ have appeared which tend to substantiate the original arguments. For example, hcp Fe-Ru, Fe-Os, and Fe-Mn alloys have antiferromagnetic transitions and extrapolation of the data to pure Fe gives a Néel temperature of 100°K and a hyperfine field of 16 kOe.²³ To our knowledge no previous low-temperature experiment on ϵ -Fe itself has been reported.

In the present study an apparatus for cooling a high-pressure Mössbauer cell was utilized to examine α - and ϵ -Fe with the ⁵⁷Fe Mössbauer nuclide serving as the probe. The pressure-temperature region covered in this experiment is indicated by the shaded area in Fig. 1. The experimental technique is described in Sec. II while the results and discussion of the search for magnetic ordering are presented in Sec. IIIA. In conjunction with the search, considerable data were accumulated on the isomer shifts and second-order Doppler shifts of α - and ϵ -Fe as well as the hyperfine field of α -Fe. In addition, evidence for the large hysteresis associated with the $\alpha \leftrightarrow \epsilon$ transformation is presented in Sec. IIID. A preliminary report of this work has been presented.²⁵

II. EXPERIMENT

The technique used to produce the high pressure is the same as that developed and described in detail by Drickamer and co-workers.^{20,26} The system utilizes supported tapered Carboly pistons. Boron and lithium hydride are used in the cell so as to provide a γ -ray window for the 14.4-keV radiation. The sample is an Fe foil of thickness 0.0025 cm. The pressure-cell loading technique has been described previously²⁷ but a few improvements have been made.²⁸

Calibration curves relating the sample pressure to the applied force were obtained by Drickamer and co-workers for this type of pressure cell using x-ray diffraction techniques.²⁶ Recently these curves have been revised somewhat²⁹ and some typical calibrations are shown in Ref. 30. As a check (and for practice), electrical resistance measurements on Bi, loaded in the same manner as a Mössbauer source, were carried out with the Bi III-Bi V resistance discontinuity known to occur

at about 75 kbar.⁵ Fe was very nice to work with because each pressure run was self-calibrating owing to the $\alpha \rightarrow \epsilon$ transition. The first onset of the ϵ -Fe Mössbauer line was taken as 115 kbar. The rate at which α -Fe transformed to ϵ -Fe with pressure was linear and the same within experimental error for all runs ($\sim 1.0\%/kbar$). The $\alpha \rightarrow \epsilon$ transformation has been found to be quite sluggish with increasing pressure in other static pressure experiments.^{1,7,20} Certainly part of the latter is due to pressure gradients but evidence is presented later which substantiates the claim⁷ that the $\alpha \rightarrow \epsilon$ transitions are pressure martensitic with a large hysteresis associated with the transformation.

The apparatus used for lowering the temperature of the specimen which is under high pressure has been described elsewhere.³⁰ Basically, a helium cryostat is brought into thermal contact with the pressure cell which is insulated by using a low-thermal-conductance-high-compressive-strength grade of fiberglass for the pressure-transmitting column. The externally applied pressure is kept constant as the temperature of the cell is lowered so that the effects of thermal expansion on the pressure calibration are kept to a minimum. One can estimate a maximum possible deviation from the room-temperature calibration of $\pm 8\%$.²⁸

The five experimental Fe sources were prepared from Armco Fe by electroplating and diffusing ⁵⁷Co according to the detailed recipe given by Stephen.³¹ The only deviations from the latter procedure were due to the small source size required for the pressure cell.²⁸ The strength of the sources varied from about 1 to 3 mCi which corresponds to a ⁵⁷Co impurity of 0.25-0.75% by weight for a source of dimensions $0.063 \times 0.038 \times 0.0025$ cm. Sodium ferrocyanide [$Na_4Fe(CN)_6 \cdot 10H_2O$ enriched to ~ 90 -at. % ⁵⁷Fe] suspended in Lucite was used as the absorber.

It is advantageous to convert the data to indicate volume variation instead of pressure variation due to the fact that most theories on solids are intimately related to the lattice constants.

The most precise measurements available on the lattice constants of α - and ϵ -Fe were obtained by Mao *et al.*³² using x-ray diffraction techniques at pressures up to 300 kbar. They found the room-temperature isotherms to closely fit the Murnaghan relations

$$(V/V_0)(bcc) = (1 + \frac{1}{275} P)^{-0.169},$$

$$V_0 = 7.093 \text{ cm}^3/\text{mole} \quad (1)$$

$$(V/V_0)(hcp) = (1 + \frac{1}{325} P)^{-0.196},$$

$$V_0 = 6.72 \text{ cm}^3/\text{mole} \quad (2)$$

The c/a ratio of ϵ -Fe was found to be constant with pressure and equal to 1.603.³³

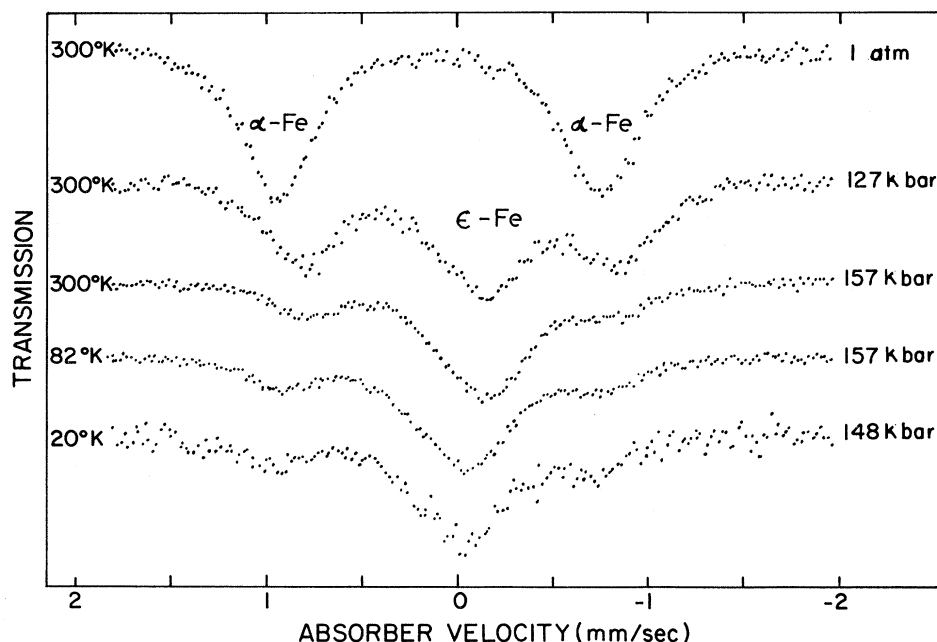


FIG. 2. Experimental Mössbauer spectra on ± 2 -mm/sec velocity scale at various combinations of pressure and temperature. The latter scale includes only the inner two lines of the usual six-line magnetic pattern of α -Fe. The typical number of counts accumulated in each channel was of the order of 50 000 to 500 000.

Thermal expansion corrections are desirable so that volume and temperature dependences exhibited by the data will be explicit. The effect of pressure on the thermal expansion of α - and ϵ -Fe has been estimated²⁸ using the Grüneisen relations, the Debye model, and the experimental temperature variation of the thermal expansion of α -Fe at normal pressure. The results of the calculation have been compared with the results of a more detailed calculation on Cu³⁴ and are found to behave qualitatively in the same manner; i. e., there is a large decrease in thermal expansion with such pressures. Using the volume corrections, the isotherms at 82 and 20 °K were constructed from the experimental 300 °K isotherms [Eqs. (1) and (2)]. Thus, when the pressure-to-volume conversion is done for each datum, the thermal expansion correction is also made by using the appropriate isotherm.

III. RESULTS AND DISCUSSION

A. Antiferromagnetism in ϵ -Fe?

Shown in Fig. 2 are a few of the experimental Mössbauer spectra obtained at various pressures and temperatures. Note that the velocity scale includes only the inner two lines of α -Fe. A hyperfine field of 16 kOe in ϵ -Fe²³ would produce a splitting of ~ 0.52 mm/sec and hence would be very apparent on the scale shown. One can see from the three lower spectra that the ϵ -Fe line apparently retains the same linewidth from 300 to 20 °K, the thermal shift being the only obvious change in the character of the spectra.

Two spectra were made near 150 kbar and 20 °K on two different Fe samples. Both yielded the same linewidth, within experimental error (± 0.02 mm/sec), as obtained at 82 and 300 °K. On a third Fe sample a thermal scan was made to 48 °K at 176 kbar (a lower temperature was not reached on this run because of a loss of thermal contact of the pressure cell with the helium cryostat). Analysis of the thermal scan data indicated no anomalous line broadening (± 0.10 mm/sec) as a function of temperature.

Hence, the data yield no temperature trend for the linewidth of the ϵ -Fe line. However, the latter was found to be definitely broader than the inner two α -Fe lines at all experimental pressures and temperatures. Figure 3 displays the linewidths (full width at half-maximum) of the inner two α -Fe lines and the single ϵ -Fe line as a function of pressure. For a given pressure the linewidths obtained at the three experimental temperatures (300, 82, and 20 °K) were averaged to give a single datum since, as mentioned above, they were the same within experimental error. The broadening is conclusive because one can see that the linewidths were obtained from samples of coexisting α - and ϵ -Fe.

The width of 0.44 mm/sec for α -Fe at atmospheric pressure is accounted for as follows: (a) 0.19 mm/sec natural linewidth; (b) 0.07 ± 0.01 mm/sec instrumental broadening; (c) 0.15 ± 0.02 mm/sec owing to the finite thickness of the absorber; and (d) 0.03 ± 0.01 mm/sec owing to self-absorption in the source. The above values were determined by using the experimental Fe sources

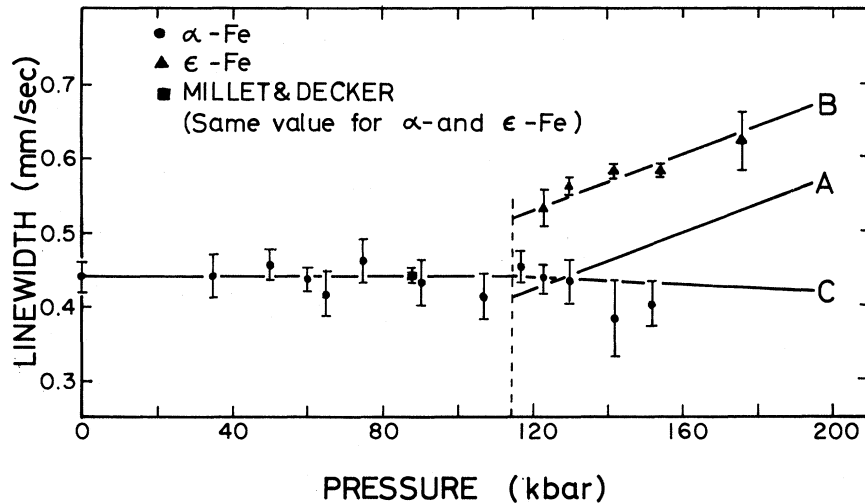


FIG. 3. Linewidths of α - and ϵ -Fe resonance lines vs pressure. Solid lines A, B, and C are discussed in the text.

and absorber in combination with various source and absorbers whose properties were already known. Thus, the linewidth obtainable in this experiment for a source of natural linewidth is 0.41 mm/sec.

There are at least three mechanisms for producing the observed broadening of the ϵ -Fe resonance line relative to the inner α -Fe lines: (i) increased self-absorption, (ii) small quadrupole interactions, and (iii) small magnetic hyperfine fields.

1. Self-Absorption

The effects of self-absorption on the experimental linewidth can easily be estimated from the calculations of Margulies *et al.*³⁵ The effective source thickness is given by

$$T_s = fn\sigma_0 t, \quad (3)$$

where f is the Mössbauer fraction (0.8 at room temperature), n is the number of atoms of ^{57}Fe per unit volume ($1.85 \times 10^{21}/\text{cm}^3$), σ_0 is the resonance cross section ($2.4 \times 10^{-18} \text{ cm}^2$), and t is the thickness of the source foils (0.0025 cm). The resulting $T_s = 8.8$ should produce a line broadening for the inner α -Fe lines of 0.02 mm/sec. This agrees with the measured values (0.03 ± 0.01 mm/sec).

If all of the α -Fe is converted to ϵ -Fe and there are no hyperfine fields in ϵ -Fe, then $T_s = 8.8$ should produce a line broadening of ~ 0.19 mm/sec and hence a linewidth of 0.60 mm/sec in this experiment. Pipkorn *et al.*,²⁰ who used sources of the same thickness, observed a slight broadening as the amount of ϵ -Fe increased and, although no quantitative experimental results were given, an expected broadening of 0.18 mm/sec for 100% ϵ -Fe was estimated, which is close to the present calculation. In this study the α -Fe transformed

to ϵ -Fe at a rate of $\sim 1\%/kbar$ and none of the samples was subjected to enough pressure to complete the transformation. There is recent evidence that the transformation is pressure martensitic.⁷ In such a case small regions (nuclei) of ϵ -Fe begin to form at the martensitic start pressure (assumed to be 115 kbar in this experiment). These nuclei grow in size and increase in number only as the pressure is increased. If the initial sizes of the nuclei are small compared to the thickness of the foil (0.0025 cm) one can estimate the expected broadening as a function of pressure for a 1% transformation rate and this is shown as line A in Fig. 3. Note that line B, having the same slope as A, gives a good fit to the experimental data and that it is displaced from line A by 0.11 mm/sec. The latter indicates, in addition to self-absorption, a contribution to the broadening which, discussed later, may come from small quadrupole interactions.

Another possibility is that the initial nuclei are not small but have sizes comparable to that of the sample thickness. The hcp line would then appear with some value owing to broadening between 0.41 and 0.60 mm/sec. To obtain some idea as to the size of the initial martensitic nuclei one can compare to the α - γ transformation. Direct experimental observation of martensitic nuclei have been made for Fe precipitates in Cu; nuclei dimensions of the order of 200 Å were observed and it was concluded that the initial size of the nucleus is only a few atoms in thickness.³⁶ We therefore assume that the additional 0.11-mm/sec broadening is not due to self-absorption.

Note (from Fig. 3) that the width of the α -Fe lines appears to decrease with increasing pressure above 115 kbar. This is consistent with the above arguments since the self-absorption in α -Fe de-

creases. This is a smaller effect than that for ϵ -Fe owing to the smaller effective thickness of the inner α -Fe lines and the expected decrease can be seen in curve C of Fig. 3.

The values for the linewidths of α - and ϵ -Fe reported by Millet and Decker²¹ (see Fig. 3) are of interest because their source was transformed completely to ϵ -Fe. The fact that the linewidths are reportedly the same within 0.01 mm/sec implies that the effective thickness of their source was less than $T_s = 0.5$, which in turn indicates an equivalent source thickness of 0.00015 cm—extremely small. No information on the thickness of their source was given, however.

2. Quadrupole Interactions

There exists an electric field gradient at each lattice site in a hexagonal structure which interacts with the quadrupole moment of the ^{57}Fe nucleus to produce a splitting of the energy levels. The electric field gradient in a hexagonal lattice is axially symmetric; hence, the asymmetry parameter is zero, and the quadrupole splitting depends only on the electric field gradient parameter³⁷:

$$q = (1 - \gamma_\infty)q_i + (1 - R)q_a. \quad (4)$$

Here q_a is the contribution from the nonsphericity of the conduction-electron distribution surrounding the ^{57}Fe atom, and q_i is the contribution from all other ions and electrons. γ_∞ and R are the Sternheimer antishielding and shielding factors which are governed by the amount of screening of the nucleus by the closed shells of inner electrons.³⁸

Rather precise methods exist for calculating q_i and, in particular, for a lattice of point charges,³⁹

$$q_i = [0.0065 - 4.3584 (c/a - 1.6333)]/a^3, \quad (5)$$

where c/a is the usual ratio of lattice constants for a hexagonal lattice. Using the experimental values³² for ϵ -Fe of $c/a = 1.603$ and $a = 2.46 \text{ \AA}$ at 145 kbar, one finds $q_i = 0.88 \times 10^{22}/\text{cm}^3$. Assuming $\gamma_\infty = -9$ ³⁸ leads to a splitting of ~ 0.03 mm/sec from q_i .

The analysis in Sec. III A 1 indicates a contribution of 0.11 ± 0.03 mm/sec to the broadening of the ϵ -Fe line in addition to that expected from increased self-absorption. If the latter is indeed from quadrupole interactions then simple analysis yields a splitting of 0.17 ± 0.03 mm/sec. Thus one can say that the magnitude of splitting caused by q_a is either 0.14 or 0.20 mm/sec because it has been shown that the q_a contribution in metals can be significantly larger in magnitude and of opposite sign to the q_i contribution.⁴⁰

A quadrupole splitting of 0.032 mm/sec has been observed for ^{57}Fe in hcp Co using the Mössbauer effect.⁴¹ Co has $c/a = 1.630$ so that q_i is an order of magnitude smaller than that of ϵ -Fe; hence, a

slight distortion of the local conduction-electron distribution away from sphericity was assumed to be the cause of the splitting. This distortion may be due to the presence of ^{57}Fe as an impurity. A study of ^{57}Fe in several hexagonal lattices⁴² finds quadrupole splittings of the order of 0.3–0.5 mm/sec, which are one or two orders of magnitude larger than the calculated contribution from q_i . The splittings are interpreted to be due to the ^{57}Fe as an impurity in the lattice, i. e., local distortion at each ^{57}Fe site. The present result indicates that even when the ^{57}Fe is not an impurity the quadrupole splitting cannot be completely accounted for by q_i .

The Mössbauer study on hcp Fe alloys predicts a quadrupole splitting of 0.14 mm/sec for ϵ -Fe.²³ No error limits were given but judging from the precision of the extrapolation one can say that this value agrees with our value within experimental error. Agreement may not necessarily be expected since one should consider that such extrapolations taken from nonpressure experiments give values which may not be valid at the pressure at which ϵ -Fe exists experimentally. Indeed, the c/a values of Fe-Mn, -Ru, and -Os apparently do not extrapolate to a unique value at 100% ϵ -Fe.²³

3. Hyperfine Field

Since the previously described mechanisms are more than sufficient to explain the observed broadening, it is unlikely that magnetic hyperfine interactions play a role, especially since the broadening is temperature independent. One can say that the hyperfine field in ϵ -Fe is 0 ± 1 kOe for all pressures and temperatures reached in this experiment. The ϵ -Fe phase was subjected to temperatures down to 20° K so that the predicted hyperfine field of 16 kOe below 100° K²³ was definitely not observed. One is thus led to the task of explaining the apparent absence of antiferromagnetism in ϵ -Fe.

The comparison of ϵ -Fe to γ -Fe in the original argument²⁰ was based on the assumption that lattice symmetry is unimportant and that nearest-neighbor distance is the property to consider. Using the relevant experimental lattice constants for α -Fe (2.866 Å at standard conditions),³² γ -Fe (3.547 Å at $T = T_N = 70^\circ \text{K}$ and 1 atm),⁴³ and ϵ -Fe (2.461 Å, $c/a = 1.603$ at room temperature and 145 kbar)³² one finds the nearest-neighbor distance in ϵ -Fe (2.431 Å) to be closer to that of α -Fe (2.482 Å) than that of γ -Fe (2.508 Å).

If one examines the Bethe-Slater curve,⁴⁴ which relates the exchange energy to the ratio of atomic separation and the diameter of the unfilled electron shell, one sees that relative to α -Fe a decrease in atomic separation leads to a decrease in the exchange energy, i. e., a tendency toward antiferro-

magnetism. Using the above atomic separations for the three phases of Fe and assuming no difference in the $3d$ shell diameter, one finds that all three phases cannot be placed on the same curve. This is not surprising since the exchange energy varies with the kind of structure and particularly with the number of nearest neighbors, so a different curve should be constructed for each structure.⁴⁵

That the Bethe-Slater curves may not be applicable to Fe in the first place can be demonstrated as follows. α -Fe is at a position on the curve where the slope is large so that the exchange energy, which is proportional to the Curie temperature T_C , should vary noticeably with lattice spacing. Experimentally, $dT_C/dP = 0 \pm 0.03$ °K/kbar!³ Although the Bethe-Slater curve has proven to be very useful for explaining properties of some metals and alloys, one should be careful in applying it to Fe. Lattice symmetry seems to be important when comparing the properties of α -, γ -, and ϵ -Fe.

What about the more direct evidence from the hcp Fe-alloy experiments which indicates $T_N = 100$ °K?²³ The latter comes from extrapolations of data in the region of 60–85-at% Fe. Apparently the extrapolations should not be linear as assumed; it should be noted, however, that pressure studies of Fe-Ru alloys in the region from 91-at.% Fe⁴⁶ indicate pressure-temperature phase diagrams very similar to the pure Fe diagram, and a linear extrapolation to pure Fe gives the same value for the triple point as found experimentally.

The c/a ratio may be the deciding factor. As mentioned earlier the c/a values for Fe-Mn, -Ru, and -Os apparently do not extrapolate to a unique value for ϵ -Fe, the three values being about 1.622, 1.611, and 1.601, respectively.²³ There appears to be a strong correlation between the Néel temperature and the c/a ratios, with Fe-Mn having the higher Néel temperatures. The experimental c/a value of 1.603 for ϵ -Fe³² is closest to that of Fe-Os, which is indeed the weakest antiferromagnet of the three. The data presented on the hcp Fe-Os alloys²³ are not very precise and the Néel temperature may be lower than 20 °K. Thus, antiferromagnetism may exist in ϵ -Fe below 20 °K, the lowest temperature to which ϵ -Fe was subjected in the present experiment.

Finally, one cannot rule out the possibility that higher pressures are required. For example, Rhiger and Ingalls⁴⁷ have experimentally observed an ordering temperature for Fe-Ni (Invar) alloys which increases with pressure, i. e., the ordering (apparently antiferromagnetic) enhanced at higher pressure.

Up to this point we have discussed the apparent absence of antiferromagnetism in ϵ -Fe. One may also be just as concerned about the absence of fer-

romagnetism in ϵ -Fe. Cubic and hexagonal Co are both ferromagnetic, so why is it that ϵ -Fe is not ferromagnetic? A possible explanation based on the band model of ferromagnetism has been suggested by Wohlfarth⁴⁸. Since there are no experimental or theoretical determinations of the density-of-states curve for ϵ -Fe, perhaps one can use the paramagnetic density-of-states curve for ϵ -Co⁴⁹ and adjust the Fermi surface for one less electron. When one does this, it is found that the density of states at the Fermi surface $n(E_F)$ is about 20% less for ϵ -Fe relative to paramagnetic ϵ -Co. The Stoner criterion for ferromagnetism is given by⁵⁰

$$S = [\Delta E / (n \uparrow - n \downarrow)] n(E_F) > 1, \quad (6)$$

where ΔE is the exchange splitting and $n \uparrow - n \downarrow$ is the difference in the number of spin-up and spin-down d electrons per atom. For ϵ -Co Wohlfarth estimates $S \approx 1.2$,⁴⁹ so that the 20% decrease in ϵ -Fe as estimated above places S very close to the critical value of 1. Remember also that the width of a band may increase as the volume decreases leading to a further reduction in $n(E_F)$ for ϵ -Fe, since its volume at 115 kbar is less than that of ϵ -Co at 1 atm. Hence S may very well be less than 1, implying that ϵ -Fe cannot be ferromagnetic.

B. Velocity Shift

The centroid of a Mössbauer spectrum may shift with temperature and pressure. There are two distinct effects causing this γ -ray energy shift: the isomer shift and the second-order Doppler shift (often referred to as the thermal shift). The former is proportional to the difference in total electron densities at the nucleus of the emitting and adsorbing nuclei, while the latter is proportional to the difference in mean-square velocities $\langle v^2 \rangle$ of the emitting and adsorbing nuclei. Provided the two contributions can be separated one may obtain information on the electronic wave functions and the lattice dynamical property $\langle v^2 \rangle$.

In this experiment only the environment of the source was changed so that one may write for the velocity shift³⁷

$$\delta = \alpha |\psi(0)|^2 - \langle v^2 \rangle / 2c + \text{const}, \quad (7)$$

where $|\psi(0)|^2$ is the total electronic density evaluated at the nucleus and α is a negative constant whose value is on the order of $(-0.3 \pm 0.1)a_0^3$ mm/sec.⁵¹

Below we present (i) the pressure and volume shifts, $\delta(P)$ and $\delta(V)$, at 82 and 300 °K and (ii) the thermal shift $\delta(T)$ as a function of volume. Only as a first approximation can one assume that the explicit volume and temperature dependence of δ is contained in $|\psi(0)|^2$ and $\langle v^2 \rangle$, respectively. A closer study of the data clearly indicates that

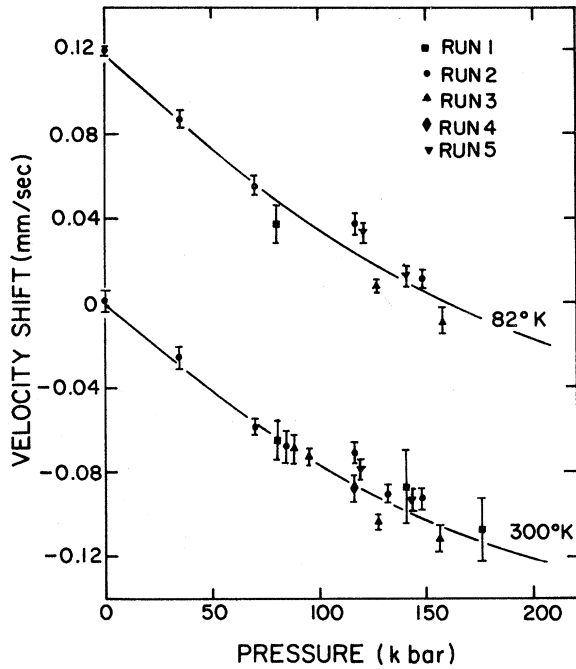


FIG. 4. Pressure dependence of the velocity shift of α -Fe. The values are presented relative to the value at 300 °K and 1 atm.

$|\psi(0)|^2$ increases with temperature and $\langle v^2 \rangle$ increases with decreasing volume.

1. Pressure and Volume Shift

a. α -Fe (bcc). The pressure dependence of the velocity shift of α -Fe is shown in Fig. 4, where δ is presented relative to its value at 300 °K and 1 atm. The error bars are those from the computer fit and do not include possible errors due to slight variations in pressure cell loading from run to run. The solid curves are least-squares fits of parabolas to the data:

$$\delta(300^\circ\text{K}) = (0 \pm 0.003) - (9.08 \pm 0.88) \times 10^{-4} P + (1.61 \pm 0.58) \times 10^{-6} P^2, \quad (8)$$

$$\delta(82^\circ\text{K}) = (0.117 \pm 0.003) - (9.48 \pm 1.14) \times 10^{-4} P + (1.41 \pm 0.82) \times 10^{-6} P^2, \quad (9)$$

where P is in kbar and δ in mm/sec. Equations (8) and (9) can be compared with previous results listed in Table I. The 300 °K curve has a slightly larger initial slope than the parabolic fit of Moyzis and Drickamer,⁵² but this is probably due to the difference in calibrations. Fitting a straight line to the data below 100 kbar gives

$$\frac{\partial \delta}{\partial P} = -(7.94 \pm 0.24) \times 10^{-4} \text{ mm/sec kbar}, \quad (10)$$

which is in agreement with all previous measurements^{20,52-54} and closest to the original and most

TABLE I. Previous high-pressure data on bcc and hcp Fe. The pressure calibration points are given since they are subject to revision as techniques improve. δ is the velocity shift and hence includes no corrections for the second-order Doppler effect. Errors are given in parentheses.

| Ref. | P_{max} (kbar) | Calibration points (kbar) | $\frac{\partial \delta}{\partial P}$ (α -Fe) (10^{-4} mm/sec kbar) | $\frac{\partial \delta}{\partial \ln V}$ (α -Fe) (mm/sec) | $\delta_0 - \delta(\epsilon\text{-Fe})$ (mm/sec) | $\frac{\partial \ln H}{\partial P}$ (α -Fe) (10^{-1} /kbar) | $\frac{\partial \ln H}{\partial \ln V}$ (α -Fe) | Comments |
|------|-------------------------|--|---|---|--|--|---|--|
| 53 | 3 | | -7.98(0.31) | | | | | |
| 62 | 10 | Manganin wire | | | | | | |
| 61 | 65 | Bi (I \rightarrow II) = 25.4 Ti (II \rightarrow III) = 36.7 Ba (I \rightarrow II) = 58.6 | | | | | | $T = 196^\circ\text{K}$ $T = 273^\circ\text{K}$ $T = 357^\circ\text{K}$ |
| 19 | 140 | Fe($\alpha \rightarrow \epsilon$) = 130 | | | | | | $\delta_0/\partial \ln V \sim 0.8$ for ϵ -Fe |
| 20 | 240 | Fe ($\alpha \rightarrow \epsilon$) = 130 | -8.3 | | | | | [nonlinear behavior] |
| 54 | 85 | Bi (I \rightarrow II) = 26 Ba (I \rightarrow II) = 57 Bi (III \rightarrow V) = 78 | -7.46(0.21) | | | | | [nonlinear behavior] $P < 60$ kbar |
| 52 | 146 | Fe ($\alpha \rightarrow \epsilon$) = 130 | [1.38(0.22) + 2.69(4.53) ΔV 1.47(0.17)] | | | | | $\delta_0 - \delta$ independent of T up to triple point Extrapolation from hcp Fe-alloy studies |
| 21 | 88 | Bi (I \rightarrow II) = 26 Bi (III \rightarrow V) = 78 | | | | | | |
| 23 | 0 | | | | | | | |

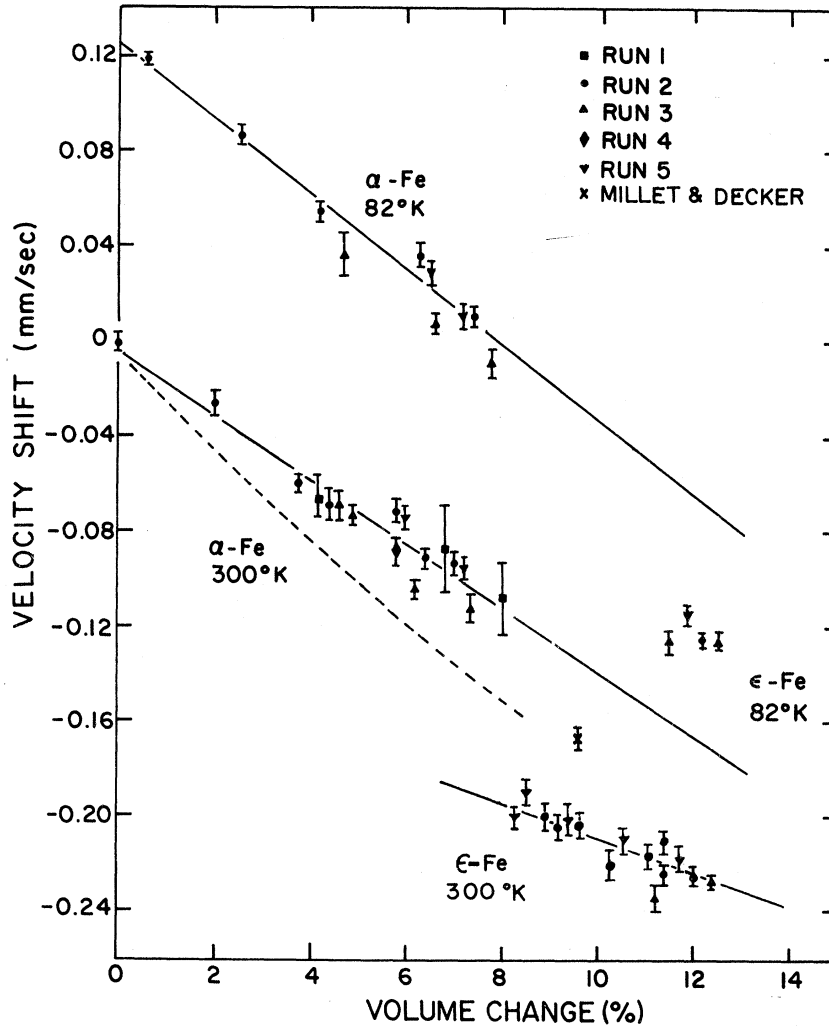


FIG. 5. Volume dependence of the velocity shift of α - and ϵ -Fe. All values are presented relative to the value for α -Fe at 300°K and 1 atm. The dashed and solid lines are discussed in the text.

precise value of Pound *et al.*⁵³

The volume dependence of the velocity shift of both α - and ϵ -Fe is shown in Fig. 5. The $\delta(V)$ data are fitted as well with straight lines as with parabolas which indicates that the curvature in $\delta(P)$ is probably due to changes in compressibility with pressure [Eq. (1)]. One finds

$$\frac{\partial \delta}{\partial \ln V} = 1.40 \pm 0.08 \text{ mm/sec at } 300^\circ\text{K}, \quad (11)$$

$$\frac{\partial \delta}{\partial \ln V} = 1.62 \pm 0.11 \text{ mm/sec at } 82^\circ\text{K}. \quad (12)$$

The contribution to $\partial \delta / \partial \ln V$ from the second term of Eq. (7) can be calculated from the Debye model

$$\langle v^2 \rangle = \frac{9k\Theta}{m} \left[\frac{1}{8} + \left(\frac{T}{\Theta} \right)^4 \int_0^{\Theta/T} \frac{x^3 dx}{e^x - 1} \right] \quad (13)$$

and the Grüneisen relation

$$\frac{\partial \ln \Theta}{\partial \ln V} = -\gamma, \quad (14)$$

where Θ is the Debye temperature and γ is the Grüneisen parameter. Assuming γ is constant with volume and temperature one finds for Θ ($P=0$) = 420°K and $\gamma=1.75$ ⁵⁵ (see the Appendix),

$$\frac{1}{2c} \frac{\partial \langle v^2 \rangle}{\partial \ln V} = -0.071 \text{ mm/sec at } 300^\circ\text{K} \quad (15)$$

$$= -0.176 \text{ mm/sec at } 82^\circ\text{K}. \quad (16)$$

Using the latter values one can correct Eqs. (11) and (12) to obtain the volume dependence of the isomer shift:

$$\frac{\alpha \partial |\psi(0)|^2}{\partial \ln V} = 1.33 \pm 0.08 \text{ mm/sec at } 300^\circ\text{K}, \quad (17)$$

$$\frac{\alpha \partial |\psi(0)|^2}{\partial \ln V} = 1.44 \pm 0.11 \text{ mm/sec at } 82^\circ\text{K}. \quad (18)$$

The volume dependence of $|\psi(0)|^2$ has been discussed previously.^{20,52,58} For example, a treatment has been made using wave functions calcu-

lated from a modified-tight-binding method in conjunction with a decomposition of the total density of states into components of s -, p -, and d -like character.⁵⁶ From the latter theory, the expected variation of the isomer shift caused by increasing only the $4s$ density at the nucleus is shown as the dashed curve in Fig. 5. The difference between the latter calculation and the experimental data has been used to deduce a relation between α [Eq. (7)] and a parameter characterizing transfer of electrons between the s and d bands.⁵² Using a recent value of $\alpha = -0.31a_0^3$ mm/sec⁵¹ leads to a small transfer from the s to the d band.

b. ϵ -Fe (hcp). The ϵ -Fe data at 300 °K are fitted with

$$\frac{\partial \delta}{\partial \ln V} = 0.84 \pm 0.15 \text{ mm/sec}, \quad (19)$$

which is in agreement with the data of Pipkorn *et al.*²⁰ Insufficient data were obtained to establish the corresponding slope at 82 °K.

The fact that the volume dependence of the velocity shift of ϵ -Fe [Eq. (19)] is significantly less than that of α -Fe [Eq. (11)] is in agreement with the findings of a systematic study of the volume dependence of the velocity shift in several transition metals⁵⁷: $\partial \delta / \partial \ln V$ is always less in the close packed structures (hcp and fcc) than that in the bcc structures. The latter has tentatively been interpreted as due to enhanced s -to- d transfer compared to bcc structures,⁵⁷ or else different shapes of $n(E_F)$.

The data of Fig. 5 clearly indicate that the electron density of the nucleus is larger in ϵ -Fe than in α -Fe at the same volume. The latter must be due to a slight difference in band structure between α - and ϵ -Fe as discussed by Pipkorn *et al.*²⁰

For comparison with previous experiments

$$\begin{aligned} \delta(\epsilon\text{-Fe}, 115 \text{ kbar}, 300^\circ\text{K}) - \delta(\alpha\text{-Fe}, 1 \text{ atm}, 300^\circ\text{K}) \\ = -0.214 \pm 0.010 \text{ mm/sec}^{-1}, \quad (20) \end{aligned}$$

$$\begin{aligned} \delta(\epsilon\text{-Fe}, 115 \text{ kbar}, 300^\circ\text{K}) - \delta(\alpha\text{-Fe}, 115 \text{ kbar}, 300^\circ\text{K}) \\ = -0.133 \pm 0.015 \text{ mm/sec}^{-1}. \quad (21) \end{aligned}$$

From Table I it is observed that both of the above values are slightly smaller in magnitude than the values reported by Pipkorn *et al.*²⁰ The value reported by Ohno²³ (see Table I) agrees with Eq. (20) but this should not be expected since the volumes of the hcp Fe-Mn, -Ru, and -Os alloys all extrapolate to values greater than those at which pure ϵ -Fe exists experimentally. From our volume dependence of the isomer shift of ϵ -Fe [Eq. (19)] we can extrapolate to the volumes of the hcp-Fe alloys and say that the alloy extrapolations should give a shift equal or smaller in magnitude than 0.17 mm/sec. Also of interest is the comparison to the result of Millet and Decker²¹ (also

see Fig. 5)

$\delta(\epsilon\text{-Fe}, 88 \text{ kbar}, \text{room temp.})$

$$\begin{aligned} -\delta(\alpha\text{-Fe}, 88 \text{ kbar}, \text{room temp.}) \\ = -0.096 \pm 0.007 \text{ mm/sec}, \quad (22) \end{aligned}$$

who claim that a pressure gradient in the Drickamer-type pressure system is responsible for the discrepancy, i. e., the α -Fe is subjected to a lower pressure than the ϵ -Fe for the same applied pressure. From the slope of Eq. (11) one can estimate that a pressure gradient of about 50% is required to bring the values into agreement. Such a gradient would produce line broadening due to velocity shifts and hyperfine fields within the sample. From Fig. 3 one can see no obvious increase of the linewidth of the α -Fe lines with pressure but due to the uncertainty in the linewidths one cannot rule out gradients of up to 30%. Even so, the latter is not sufficient to resolve the discrepancy.

2. Temperature Shift

The effect of pressure on the temperature shift is demonstrated by the experimental data in Fig. 6, where each datum corresponds to the shift from 300 to 82 °K (corrected for thermal contraction) at a particular volume. The dashed line is a least-squares fit to the data.

Using Eqs. (13) and (14) one can calculate the second-order Doppler shift from 300 to 82 °K as a function of volume using $\Theta(P=0) = 420$ °K and $\gamma = 1.75$ and this is shown as the solid line in Fig. 6. If one tries to be more careful by using the experimental phonon frequency distribution⁵⁸ instead of the Debye distribution, one finds qualitatively that the Doppler shift is even smaller so that the experimental data would lie even further from the calculated values. The explanation lies in the small explicit temperature dependence of the isomer shift. Using the value found by Housley and Hess⁵⁹

$$\begin{aligned} \frac{\alpha \partial |\psi(0)|^2}{\partial T} \approx -2.7 \times 10^{-5} \text{ mm/sec}^\circ\text{K} \\ (T < \sim 700^\circ\text{K}), \quad (23) \end{aligned}$$

one obtains a correction to the 300–82 °K shift of -0.006 mm/sec at atmospheric pressure. Assuming the correction to be volume independent, then the data are brought into closer agreement with the expected second-order Doppler shift (solid line). The similarities of the experimental and theoretical slopes in Fig. 6 reflect the validity (although not too precisely) of the Grüneisen relation [Eq. (14)].

The effect of pressure on the second-order Doppler shift can also be demonstrated as in Fig. 7, where use is made of some additional data at 20 °K. The α -Fe temperature shift (corrected for thermal expansion and the temperature-dependent isomer

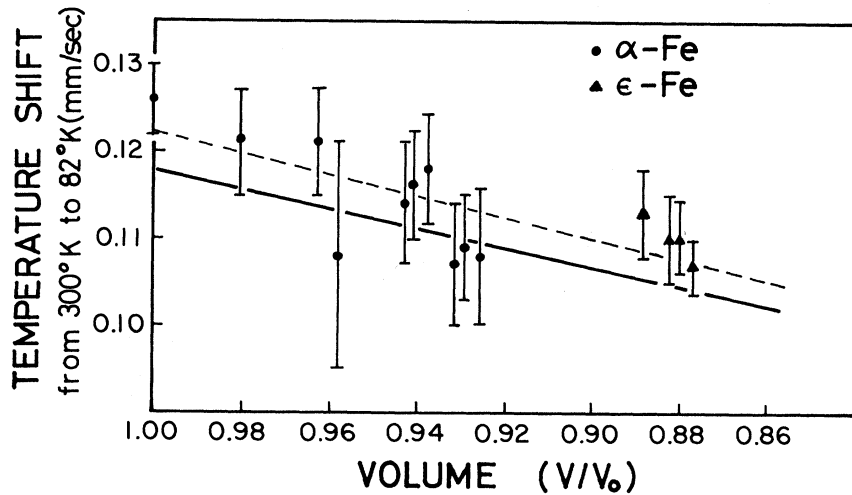


FIG. 6. Volume dependence of the temperature shift from 300 to 82°K. The dashed and solid lines are discussed in the text. V_0 is the volume at 300°K and 1 atm.

shift) at $P=0$ is best fitted with a Debye curve [Eq. (13)] with $\Theta=410^\circ\text{K}$. The ϵ -Fe temperature shift (also corrected) at $P \approx 145$ kbar is best fitted with $\Theta=545^\circ\text{K}$. The latter indicates an increase in the zero-point mean-squared velocity of 33%.

Specific-heat measurements on a series of hcp Fe-Ru alloys have been used to deduce the only other reported Debye temperature for ϵ -Fe of 385°K by extrapolating the results to 100% Fe.⁶⁰ In the same study the Debye temperature of α -Fe was found to be 432°K. The measurements were made over the range from 300 to 60°K—very similar to the temperatures covered in the present experiment. In order to compare, the present value for ϵ -Fe of 545°K can be corrected to the $P=0$ value using Eq. (14) with $\gamma=1.75$. The result is $\Theta(P=0)=448^\circ\text{K}$, which is in significant disagreement with the 385°K value from the specific-heat measurements. Note that the present result is consistent with the total volume change of 12% (from α -Fe at $P=0$ kbar to ϵ -Fe at $P=145$ kbar) which should produce a change in Θ from 420 to 525°K according to Eq. (14). Here, as earlier, we find a discrepancy between values of properties predicted by extrapolation of alloy results and direct measurements.

C. Hyperfine Field of α -Fe

Shown in Fig. 8 are the results on the pressure and volume variation of the hyperfine field H of α -Fe at 300 and 82°K. The straight lines are least-squares fits with slopes

$$\frac{\partial \ln H}{\partial P} = -1.66 \pm 0.12 \times 10^{-4} \text{ kbar}^{-1} \text{ at } 300^\circ\text{K}, \quad (24)$$

$$\frac{\partial \ln H}{\partial P} = -1.62 \pm 0.12 \times 10^{-4} \text{ kbar}^{-1} \text{ at } 82^\circ\text{K}, \quad (25)$$

$$\frac{\partial \ln H}{\partial \ln V} = 0.372 \pm 0.026 \text{ at } 300^\circ\text{K}, \quad (26)$$

$$\frac{\partial \ln H}{\partial \ln V} = 0.353 \pm 0.026 \text{ at } 82^\circ\text{K}, \quad (27)$$

where H and V are normalized to their values at 300°K and 1 atm. The pressure variation is in agreement with all previous results (see Table I). Closest agreement is with the results of the NMR experiments,^{61,62} which are the only studies which have been done at temperatures other than room temperature. Their slopes at 196, 273, and 357°K are the same within experimental error.

The small change in the hyperfine field (2.5%) upon cooling to 82°K is due to the fact that at 300°K, H is 97% of its saturation value of 339 kOe. Due to the near saturation and the very small pressure dependence of H , the slopes at 300 and 82°K should be nearly the same as indeed the results indicate.

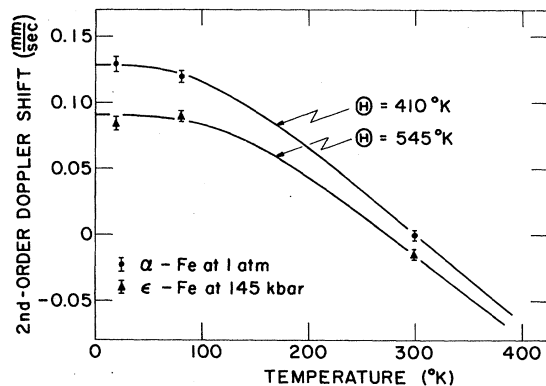


FIG. 7. Second-order Doppler shift of α - and ϵ -Fe. The solid lines are Debye curves for the characteristic temperatures (Θ) shown. The values are presented relative to α -Fe at 300°K and atmospheric pressure, and the volume contribution to the shift of ϵ -Fe at 145 kbar relative to α -Fe at atmospheric pressure has been subtracted in order to more clearly demonstrate the effect.

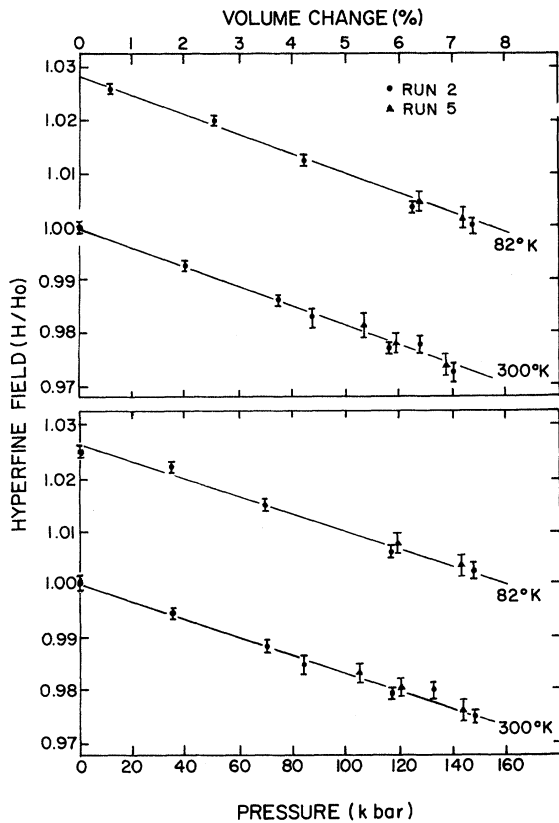


FIG. 8. Pressure and volume dependence of the hyperfine field of α -Fe. The hyperfine field and the volume are normalized to their values at 300 °K and 1 atm.

Of recent interest is the controversy over the role of the conduction electrons in contributing to the hyperfine field in α -Fe. The experimental pressure dependence of H has been used by Anderson⁶³ to deduce that the $4s$ electrons are polarized negatively (i. e., opposite to the d electron). In a recent band structure calculation by Duff and Das¹⁰ the $4s$ were found to have a net positive polarization. The latter is supported by good agreement between the theoretical and measured quantities, namely, charge and spin densities, the isomer shift, and the hyperfine field. Anderson assumed that pressure would have no effect on the compact d bands but the calculations of Duff and Das indicate that pressure may significantly widen the d bands. Thus, they postulate there is competition between an increased core polarization due to pressure-widened d bands and positive contribution from the s -like states, the net result being a decrease in the magnitude of H with pressure. Recently, the problem has been carefully treated by Stearns,⁶⁴ who shows that $\partial \ln H / \partial \ln V$ depends on many more quantities than the hyperfine field constant, and saturation magnetization as is usual-

ly assumed.^{62, 63} She also finds a net positive contribution from the conduction electrons.

D. Evidence for Hysteresis

The $\alpha \rightarrow \epsilon$ transformation has recently been reported to be pressure martensitic with a large hysteresis.⁷ The α and ϵ phases were found to coexist over a range of more than 100 kbar. Other recent evidence comes from shock-wave studies of Fe-Mn alloys.⁶⁵ Presented below are similar findings from the present experiment.

Note (in Fig. 5) that there are several ϵ -Fe data points below a volume change of 10.7%, which corresponds to 115 kbar for ϵ -Fe. These data were obtained as follows: After reaching the highest pressure allowed by the compressive strength of the fiberglass disks on runs 2 and 5, the pressure was released and a series of spectra were obtained at various applied pressures on the way down. The velocity shift of α -Fe was used as a marker such that the sample pressure was obtained from the 300 °K fit to α -Fe in Fig. 5. The ϵ phase persisted to pressures indicated by the α -Fe marker of < 60 kbar. As mentioned earlier, a pressure gradient of up to 30% cannot be ruled out but the latter is not sufficient to explain the apparent persistence of ϵ -Fe to < 60 kbar. Note also in Figs. 5 and 8 that there is considerable data presented on α -Fe above 115 kbar, the start pressure for the transformation. Although not clear in the velocity-shift data (Fig. 5), the hyperfine field (Fig. 8) appears to continue changing linearly above 115 kbar—a strong indication that the α -Fe actually exists at pressures greater than 115 kbar.

On two runs the sample was subjected to just enough pressure to start the transformation (see the spectra in Fig. 2 for $P=117$ kbar) after which the sample was cooled to 82 °K. According to Fig. 1, the α - ϵ phase boundary has a slightly negative slope in this temperature region, so that if no hysteresis exists the ϵ -Fe should revert to the α -phase. On both runs the amount of ϵ -Fe remained the same as determined by the area of the ϵ -Fe line relative to that of the α -Fe lines. The possibility of a local pressure increase upon cooling is not likely.²⁸

Finally, it was noted that the $\alpha \rightarrow \epsilon$ transformation rate was the same within experimental error for all of the experimental runs ($0.9 \pm 0.1\%$ per kbar). This is noteworthy because the Fe samples were of various dimensions—from $0.102 \times 0.038 \times 0.0025$ cm to $0.038 \times 0.038 \times 0.0025$ cm. If a large pressure gradient exists then it seems likely that samples of different sizes would transform at different rates, contrary to what has been observed.

IV. CONCLUSIONS

hcp Fe is paramagnetic to 20 °K at 148 kbar and 48 °K at 176 kbar ($H=0 \pm 1$ kOe). The temperature-

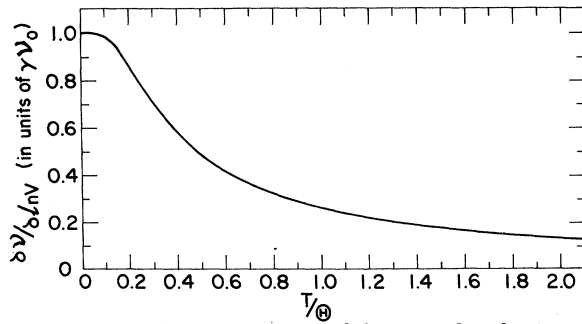


FIG. 9. Volume dependence of the second-order Doppler shift based upon the Debye model and Grüneisen relation.

independent broadening of the hcp resonance line is attributed to increased self-absorption and a small quadrupole splitting. The latter is 0.17 ± 0.03 mm/sec and independent of pressure within experimental error.

Values of the volume coefficients of the isomer shift and hyperfine field of bcc Fe have been obtained at 82 °K. The room-temperature coefficients are in agreement with previous experiments.

The effects of pressure on the second-order Doppler shift have been clearly observed while offering at the same time a fairly direct test of the validity of the Grüneisen relation. hcp Fe has a Debye temperature of 545 ± 25 °K at ~ 145 kbar, while the value for bcc Fe is 410 ± 25 °K at 1 atm.

The small increase in the electron density at the nucleus with temperature has been observed.

In addition the data substantiate other findings of an unusually large pressure hysteresis associated with the bcc \leftrightarrow hcp transformation.

ACKNOWLEDGMENTS

The authors are very grateful to Professor H. Shechter, Dr. G. A. Erickson, D. R. Rhiger, C. D. West, and G. Garcia for assistance with various phases of this work and to Professor H. G. Drickamer, Professor E. P. Wohlfarth, and Professor U. Gonser for helpful discussions.

APPENDIX

The following method was used to calculate the volume coefficient of the second-order Doppler

shift ($\partial\nu/\partial \ln V$). The formulas and graph presented can be used for a general Mössbauer isotope in a general solid.

Using Eqs. (13) and (14) one obtains (in units of velocity)

$$\frac{\partial\nu}{\partial \ln V} = \gamma\nu_0 \left[1 + \frac{8}{e^{\Theta/T} - 1} - 24 \left(\frac{T}{\Theta} \right)^4 \int_0^{\Theta/T} \frac{x^3 dx}{e^x - 1} \right], \quad (\text{A1})$$

where

$$\nu = -\frac{\langle v^2 \rangle}{2c}, \quad \nu_0 = 9k\Theta/16mc. \quad (\text{A2})$$

In cases where the Mössbauer nucleus is an impurity in a host lattice, Θ is given in the first approximation by⁶⁶

$$\Theta = \Theta_{\text{host}} (m_{\text{host}}/m)^{1/2}, \quad (\text{A3})$$

where m_{host} and m are the atomic mass of the host lattice atoms and the impurity (source or absorber) atoms.

Utilizing tabulated Debye integrals,⁶⁷ $\partial\nu/\partial \ln V$ is calculated from Eq. (A1) and shown in Fig. 9 in units of $\gamma\nu_0$. At high temperature $\partial\nu/\partial \ln V$ approaches 0 (although rather slowly, having a value of $0.027\gamma\nu_0$ at $T/\Theta = 10$).

Thus, provided one knows γ and Θ_{host} , the contribution from ν to the total velocity shift in high-pressure experiments may be quickly estimated from Eqs. (A2) and (A3) and Fig. 9. As examples consider ⁵⁷Fe in Fe and Au and ¹¹⁹Sn in Sn.

(i) ⁵⁷Fe in Fe. $\gamma = 1.75$ and $\Theta_{\text{host}} = 420$ °K⁵⁵ gives $\nu_0 = 0.114$ mm/sec and $\partial\nu/\partial \ln V = 0.176$ mm/sec at 82 °K. Note that the latter is 11% of the observed experimental result [Eq. (12)].

(ii) ⁵⁷Fe in Au. $\gamma = 2.9$ ⁶⁸ and $\Theta_{\text{host}} = 162$ °K⁶⁹ gives $\nu_0 = 0.083$ mm/sec and $\partial\nu/\partial \ln V = 0.063$ mm/sec at 300 °K, which is 16% of the observed effect.⁵⁷

(iii) ¹¹⁹Sn in Sn. $\gamma = 2.0$ (assumed) and $\Theta_{\text{host}} = 199$ °K⁶⁹ gives $\nu_0 = 0.079$ mm/sec and $\partial\nu/\partial \ln V = 0.039$ mm/sec at 300 °K, which is 4% of the observed effect.⁷⁰

The calculations indicate that the role of the second-order Doppler shift in high-pressure experiments may be significant in some cases, especially since low temperatures are now accessible and techniques will undoubtedly improve, leading to more accurate results at very high pressures.

*Work supported by the U. S. Atomic Energy Commission under Contract No. AT(45-1)-2225.

†Present address: Institut für Metallphysik and Metallkunde, Universität des Saarlandes, Saarbrücken, Germany.

‡Permanent address: Soreq Nuclear Research Center, Yavne, Israel.

§Address for the 1972-1973 academic year: University of Groningen, Groningen, The Netherlands.

¹F. P. Bundy, J. Appl. Phys. **36**, 616 (1965).

²P. C. Johnson, B. A. Stein, and R. S. Davis, J. Appl. Phys. **33**, 557 (1962).

³J. M. Leger, C. Susse, and B. Vodar, Solid State Commun. **4**, 503 (1966).

⁴L. F. Vereshchagin, A. A. Semerchan, N. N. Kuzin, and Yu A. Sadkov, Dokl. Akad. Nauk SSSR **185**, 785 (1969) [Sov. Phys. Doklady **14**, 340 (1969)].

⁵H. G. Drickamer, Rev. Sci. Instr. **41**, 1667 (1970).

- ⁶H. Mii, I. Fujishiro, and T. Nomura, *Les Propriétés Physiques Des Solides Sous Pression* (Centre National de la Recherche Scientifique, Paris, 1970).
- ⁷P. M. Giles, M. H. Longenbach, and A. R. Marder, *J. Appl. Phys.* **42**, 4290 (1971).
- ⁸S. Wakoh and J. Yamashita, *J. Phys. Soc. Japan* **25**, 1272 (1968).
- ⁹K. J. Duff and T. P. Das, *Phys. Rev. B* **3**, 192 (1971).
- ¹⁰K. J. Duff and T. P. Das, *Phys. Rev. B* **3**, 2294 (1971).
- ¹¹U. Gonser, C. J. Meechan, A. H. Muir, and H. Wiedersich, *J. Appl. Phys.* **34**, 2373 (1963).
- ¹²G. J. Johanson, M. B. McGirr, and D. A. Wheeler, *Phys. Rev. B* **1**, 3208 (1970).
- ¹³Clyde Kimball, W. D. Berber, and Anthony Arrott, *J. Appl. Phys.* **34**, 1046 (1963).
- ¹⁴R. Nathans and S. J. Pickart, *J. Phys. Chem. Solids* **25**, 183 (1964).
- ¹⁵Y. Ishikawa, Y. Endoh, and T. Takimoto, *J. Phys. Chem. Solids* **31**, 1225 (1970).
- ¹⁶L. D. Flansburg and N. Hershkowitz, *J. Appl. Phys.* **41**, 4082 (1970).
- ¹⁷Leonard Kleinman and Robert Shuntleff, *Phys. Rev. B* **4**, 3284 (1971); **3**, 2418 (1971), and references therein.
- ¹⁸S. Asano and J. Yamashita, *J. Phys. Soc. Japan* **31**, 1000 (1971).
- ¹⁹M. Nicol and G. Jura, *Science* **141**, 1035 (1963).
- ²⁰D. N. Pipkorn, C. K. Edge, P. Debrunner, G. De Pasquali, H. G. Drickamer, and H. Frauenfelder, *Phys. Rev.* **135**, A1604 (1964).
- ²¹L. E. Millet and D. L. Decker, *Phys. Letters* **29A**, 7 (1969).
- ²²H. Fujimori and H. Saito, *J. Phys. Soc. Japan* **26**, 1115 (1969).
- ²³H. Ohno, *J. Phys. Soc. Japan* **31**, 92 (1971).
- ²⁴H. Ohno and M. Mekata, *J. Phys. Soc. Japan* **31**, 102 (1971).
- ²⁵D. L. Williamson, S. Bukshpan, R. Ingalls, *Bull. Am. Phys. Soc.* **16**, 850 (1971).
- ²⁶P. Debrunner, R. W. Vaughan, A. R. Champion, J. Cohen, J. Moyzis, and H. G. Drickamer, *Rev. Sci. Instr.* **37**, 1310 (1966).
- ²⁷D. N. Pipkorn, thesis (University of Illinois, 1964) (unpublished).
- ²⁸D. L. Williamson, thesis (University of Washington, 1971) (unpublished).
- ²⁹H. G. Drickamer (private communication).
- ³⁰D. L. Williamson, S. Bukshpan, R. Ingalls, and H. Schechter, *Rev. Sci. Instr.* **43**, 194 (1972).
- ³¹J. Stephen, *Nucl. Instr. Methods* **26**, 269 (1964).
- ³²H. Mao, W. A. Bassett, and T. Takahashi, *J. Appl. Phys.* **38**, 272 (1967).
- ³³An earlier work [R. L. Clendenen and H. G. Drickamer, *J. Phys. Chem. Solids* **25**, 865 (1964)] had indicated a pressure dependence of c/a . The discrepancy is now resolved: T. Takahashi, W. A. Bassett, and H. Mao, *J. Geophys. Res.* **73**, 4723 (1968).
- ³⁴David J. O'Keefe, *J. Appl. Phys.* **41**, 5101 (1970).
- ³⁵S. Margulies and J. R. Ehrman, *Nucl. Instr. Methods* **12**, 131 (1961); S. Margulies, P. Debrunner, and H. Frauenfelder, *ibid.* **21**, 217 (1963).
- ³⁶K. E. Easterling and G. C. Weatherly, *Acta Met.* **17**, 845 (1969).
- ³⁷See, for example, *An Introduction to Mössbauer Spectroscopy*, edited by L. May (Plenum, New York, 1971).
- ³⁸R. M. Sternheimer, *Phys. Rev.* **146**, 140 (1966).
- ³⁹T. P. Das and M. Pomerantz, *Phys. Rev.* **123**, 2070 (1961).
- ⁴⁰R. E. Watson, A. C. Gossard, and Y. Yafet, *Phys. Rev.* **140**, A375 (1965).
- ⁴¹G. J. Perlow, C. E. Johnson, and W. Marshall, *Phys. Rev.* **140**, A875 (1965).
- ⁴²S. M. Qaim, *J. Phys. C* **2**, 1434 (1969).
- ⁴³Larry Kaufman and A. E. Ringwood, *Acta Met.* **9**, 941 (1961).
- ⁴⁴R. M. Bozorth, *Bell System Tech. J.* **19**, 1 (1940).
- ⁴⁵R. M. Bozorth, *Ferromagnetism* (Van Nostrand, Princeton, N. J., 1951), p. 444.
- ⁴⁶L. D. Blackburn, Larry Kaufman, and Morris Cohen, *Acta Met.* **13**, 533 (1965).
- ⁴⁷David R. Rhiger and R. Ingalls, *Phys. Rev. Letters* **28**, 749 (1972).
- ⁴⁸E. P. Wohlfarth (private communication).
- ⁴⁹E. P. Wohlfarth, *J. Appl. Phys.* **41**, 1205 (1970).
- ⁵⁰Edmund C. Stoner, *Rept. Progr. Phys.* **11**, 43 (1946-47).
- ⁵¹T. K. McNab, H. Micklitz, and P. H. Barrett, *Phys. Rev. B* **4**, 3787 (1971), and references therein.
- ⁵²J. A. Moyzis and H. G. Drickamer, *Phys. Rev.* **171**, 389 (1968).
- ⁵³R. V. Pound, G. B. Benedek, and R. Drever, *Phys. Rev. Letters* **7**, 405 (1961).
- ⁵⁴W. H. Southwell, D. L. Decker, and H. B. Van Fleet, *Phys. Rev.* **171**, 354 (1968).
- ⁵⁵G. K. White, *Proc. Phys. Soc. (London)* **86**, 159 (1965).
- ⁵⁶R. Ingalls, *Phys. Rev.* **155**, 157 (1967).
- ⁵⁷R. Ingalls, H. G. Drickamer, and G. De Pasquali, *Phys. Rev.* **155**, 165 (1967).
- ⁵⁸J. Bergsma, C. van Dijk, and D. Tocchetti, *Phys. Letters* **24A**, 270 (1967).
- ⁵⁹R. M. Housley and F. Hess, *Phys. Rev.* **164**, 340 (1967).
- ⁶⁰G. L. Stepakoff and L. Kaufman, *Acta Met.* **16**, 13 (1968).
- ⁶¹J. D. Litster and G. B. Benedek, *J. Appl. Phys.* **34**, 688 (1963).
- ⁶²G. B. Benedek and J. Armstrong, *J. Appl. Phys. Suppl.* **32**, 106S (1961).
- ⁶³D. H. Anderson, *Solid State Commun.* **4**, 189 (1966).
- ⁶⁴Mary Beth Stearns, *Phys. Rev. B* **4**, 4081 (1971).
- ⁶⁵Aristos Christou and Norman Brown, *J. Appl. Phys.* **42**, 4160 (1971).
- ⁶⁶H. J. Lipkin, *Ann. Phys. (N. Y.)* **23**, 28 (1963).
- ⁶⁷*Handbook of Mathematical Functions*, edited by M. Abramowitz and I. Stegun (U. S. Department of Commerce, Natl. Bur. Std., U. S. GPO, Washington, D. C., 1964).
- ⁶⁸P. K. Sharma and Narain Singh, *Phys. Rev. B* **1**, 4635 (1970).
- ⁶⁹C. Kittel, *Introduction to Solid State Physics*, 3rd ed. (Wiley, New York, 1967).
- ⁷⁰V. N. Panyushkin, *Fiz. Tverd. Tela* **10**, 1915 (1968) [*Sov. Phys. Solid State* **10**, 1515 (1968)].